Arabian Journal of Chemistry (2020) **13**, 6977–6985

King Saud University

Arabian Journal of Chemistry

www.ksu.edu.sa
www.sciencedirect.com

ORIGINAL ARTICLE

Synthesis and characterization of a novel controlled release nitrogen-phosphorus fertilizer hybrid nanocomposite based on banana peel cellulose and layered double hydroxides nanosheets

Sayed Majid Lohmousavi, Hossein Heidari Sharif Abad *, Ghorban Noormohammadi, Babak Delkhosh

Department of Agronomy, Science and Research Branch, Islamic Azad University, Tehran, Iran

Received 31 December 2019; accepted 29 June 2020
Available online 9 July 2020

KEYWORDS

Banana peel cellulose;
LDH nanosheets;
Hybrid nanocomposite hydrogel;
Controlled release fertilizer

Abstract In the present study, a novel environment-friendly hybrid nanocomposite of Banana Peel Cellulose-g-poly(acrylic acid)/PVA (BPC-g-PAA/PVA) hydrogel and Layered double hydroxides (LDH) nanosheets was developed using *in situ* graft polymerization for slow release of NP (nitrogen, phosphorous) fertilizers and water retention. The hybrid nanocomposite hydrogel containing NP fertilizers was characterized using FTIR, and SEM. The effects of pH changes and different saline solutions on the swelling behavior, fertilizer release and water retention properties of the nanocomposite were investigated.

The nanocomposite hydrogel showed a pH dependent swelling, as in the pH range of 7–10, the hydrogel had higher water absorbency. However, pH had opposite effects on the release of fertilizers. Phosphorus release had an increasing trend from pH 2 to 7 and it reached its maximum value at normal pH while nitrogen had a higher release rate at acidic pH and by increasing pH from 2 to 7, the release of nitrogen decreased gradually. Water absorption and fertilizer release of hydrogel was influenced by different cations in the order of $Ca^{2+} < K^{+} < Na^{+}$. Water retention study in loamy sand soil showed that the nanocomposite hydrogel significantly improved the water retention of the soil for a longer period of time, compared to neat BPC-gPAA. This result indicated that incorporation of LDH nanosheets in hydrogel matrix improved its water retention property. The obtained results revealed that the nanocomposite of BPC-g-PAA/PVA hydrogel and LDH nanosheets can be

* Corresponding author.
E-mail address: hosseinheidari97@yahoo.com (H.H.S. Abad).
Peer review under responsibility of King Saud University.

Production and hosting by Elsevier

https://doi.org/10.1016/j.arabjc.2020.06.042

a promising controlled release fertilizer formulation with enhanced water retention properties for agricultural applications.

1. Introduction

In the past decades, diminishing arable land along with the exponential growth of population have increased the demand for excessive application of fertilizers and water (Obermeier et al., 2020; Díaz-Pinés et al., 2017; Pu et al., 2011; Ros et al., 2016). However, water deficiency and environmental pollution due to the enormous utilization of fertilizers have become a series challenge in modern agriculture (Erisman et al., 2007; Li & Wu, 2008; Li et al., 2018; Xu et al., 2019). Therefore, developing formulations with slow/controlled–release fertilizer (SRF or CRF) and water retention properties is one of the important concerns in agricultural science. The use of superabsorbent hydrogels for incorporating fertilizers is an ideal alternative for preventing the loss of fertilizers during irrigation and improving water retention of soils resulting in cost effective crop production with less environmental pollution and irrigation frequency (González et al., 2015; Majeed et al., 2015; Sun et al., 2016).

Superabsorbent hydrogels have a 3D cross-linked matrix structure and contain hydrophilic functional groups which provide the hydrogel the capability to absorb and retain a large amount of aqueous solutions (Peng et al., 2016; Guilherme et al., 2015). Superabsorbent hydrogels depending on their composition also have the ability to release their water content in a sustained or controlled manner. Therefore, fertilizer encapsulated hydrogels have gained a great attention in agriculture and horticulture, especially in dry regions with non-arable lands, for reducing irrigation frequency and water consumption and enhancing the nutrition retention of soil (Essawy et al., 2016; Dai & Huang, 2017; McLaughlin et al., 2018).

Superabsorbent hydrogels obtained from graft polymerization of cellulose with acrylic acid (AA) monomers have found several applications in agriculture owing to their water absorption and retention properties and being environment friendly (Fekete et al., 2016; Fekete et al., 2017; Salmawi et al., 2018). However, their wide use in agriculture has remained limited due to low mechanical properties and high production cost (Mahfoudhi & Boufi, 2016; You et al., 2016). In this study, banana peel cellulose (BPC) which is obtained from a cheap abundant source of cellulose was used to diminish those problems (Tibolla et al., 2017). Banana peel (BP) which contains about 50% of natural cellulose and hemicelluloses, has a significant amount of functional groups including hydroxyls making it suitable for hydrogels preparation by triggering chemical reactions such as copolymerization, etherification and esterification (Tibolla et al., 2018).

To improve the mechanical properties of hydrogels, several studies suggested blending with linear or branched macromolecules and forming a semi-interpenetrating polymer network (semi-IPN) (Thompson et al., 2019; Rassu et al., 2017). In this work, poly(vinylalcohol) (PVA) was used in the semi-IPN as water soluble linear nonionic macromolecule (Wang et al., 2019). Additionally, the mechanical strength of hydrogels could be improved by adding low cost inorganic nanoparticles including nanoclays, nanosilica and layered double hydroxide (LDH) nanoparticles (Yao et al., 2016; Lewandowska-Łańcucka et al., 2015).

Layered double hydroxide (LDH) is a type of natural and synthetic clay materials which has anion exchange capacity. Thus, soil anions can be easily exchange with intercalated anions of LDH (Mishra et al., 2018). LDH has found several applications in different industries (Gao et al., 2017; Tian et al., 2015; Arif et al., 2020; Gao & Yan, 2018) due to its interesting properties such as biocompatibility, being environmental-friendly, availability and low production cost (Saiah et al., 2009; Wang & O'Hare, 2012). LDH can be used as a cost effective water absorbent or carrier for nutrients, plant hormones, pesticides and soil fertilizers in a pure form or organic–inorganic composite formulation (Bernardo et al., 2017; Hatami et al., 2018). Incorporation of LDH nanoclays in hydrogel composition can improve its fertilizer loading capacity, water absorbency, physical and mechanical properties (Hibino, 2010).

The aim of this study was to develop a novel CRF formulation based on BPC-g-poly(AA)/PVA/LDH nanocomposite. The nanocpmposite hydrogel was prepared via graft solution polymerization and was characterized using FTIR and SEM analysis. The swelling behavior and fertilizer release of prepared CRF formulation was evaluated at different pHs and saline solutions. Also, the effect of the nanocomposite hydrogel with and without PVA and LDH on water retention of sand soil was investigated.

2. Material and methods

Acyclic acid (AA), polyvinyl alcohol (PVA, Mw 25,000–30,000), potassium hydroxide (KOH), dipotassium hydrogenphosphate (K_2HPO_4), sodium sulfite (Na_2SO_3), potassium persulfate ($K_2S_2O_8$), and ammonium ceriumnitrate ($(NH4)_2Ce(NO_3)_6$) were of analytical grade and were obtained from Merck company. Banana Peel (BP) was gained from a local supplier (Tehran, Iran). All the experiments including solution preparation, swelling and fertilizer release was performed using distilled water.

2.1. Preparation of LDH nanoparticles

Chloride form of Mg-Al LDHs with the M^{2+}:M^{3+} ratio of 4:1 was prepared using coprecipitation method (Olfs et al., 2009). To do so, 300 mL of 1 M chloride salt solution containing divalent and trivalent cations and 300 mL of 1 M NaOH–NaCl were added simultaneously to 150 mL of distilled deionized water at 80 °C and stirred for 2 h. The pH of final solution was adjusted at 10 using 2 M NaOH solution. The slurry was kept at 70 °C for additional 24 h, then it was filtered. The

obtained the LDH nanoparticles were washed and dried at 70 °C.

2.2. Preparation of banana peel cellulose (BPC)

Fresh Yellow banana peels (BP) were washed to remove the dust and impurities, and then dried at 55 °C in an oven for 10 h. The dried banana peels were crushed and sieved using a 40 mesh. Then, 100 g of the banana peels powder was soaked in ethanol/toluene (100:100) mL for 24 h to remove the fat. In the next step, to remove lignin and hemicellulose, the defatted powder was soaked in 250 mL of NaOH (4% w/v) solution and stirred for 10 h. Then, the samples were filtered using Whatman paper No.4 and washed with distilled water and dried at 80 °C for 5 h.

For bleaching the cellulose, the banana peel powder was added to 20% hydrogen peroxide solution and stirred for 3 h at 85 °C. Finally, the bleached banana peel cellulose powder was filtered and washed with distilled water for several times and dried at 50 °C in a hot air oven for 10 h.

2.3. Preparation of banana peel cellulose-g-PAA/PVA/LDH/NP hybrid nanocomposite

Nitrogen/Phosphorous (NP) containing BPC-g-PAA/PVA/LDH hydrogel was prepared via graft solution polymerization (Nath & Dolui, 2018). Briefly, 100 mL of BPC mixture in distilled water (3.5 mg/ml) was poured into a three necked round-bottomed flask and stirred at 50 °C for 10 min. Then, 3 g PVA and 1.0 g LDH nanoparticles, 10.0 g urea, 5.0 g ammonium dihydrogen phosphate were added to the BPC solution while stirring. Then, 30.0 g of 70% neutralized AA and 0.15 g APS (initiator agent) were added to the mixture and nitrogen was purged to remove the dissolved oxygen. After 10 min, 0.055 g MBA (cross-linker agent) was added to the reaction mixture and temperature was raised to 60 °C. To complete the polymerization process, the stirring was continued for additional 4 h. The unreacted species were removed by immersing the nanocomposite hydrogel product in ethanol for 12 h. Then, the nanocomposite hydrogel was dried at 70 °C for 24 h and milled and sieved using a 40 mesh. Other formulations of hydrogel including BPC-g-PAA and BPC-g-PAA/PVA were also synthetized as control samples to be compared with the nanocomposite hydrogel and identify the effect PVA and LDH on water retention properties of hydrogel.

3. Structural characterization

The XRD pattern of the Mg-Al LDH nanosheets was recorded using D5000 X-ray diffractometer (Siemens, Germany) with Cu Kα radiation at 40 kV, 30 mA and scan speed of 5°/min within the range of 2θ = 2°–70°.

The FTIR analysis was used to identify the functional groups and chemical bonds of BPC and BPC-gPAA/PVA/LDH/NP (Bruker Tensor 27 FTIR Spectrometer). The analysis was performed within the wavenumber range of 400–4000 cm^{-1} using KBr pellets method.

The surface morphology of the samples was observed using a scanning electron microscope (S520 SEM, Hitachi, Tokyo, Japan).

3.1. Swelling behavior at various pHs and salt solutions

To evaluate the swelling behavior of product at various pHs, different aqueous solutions with desired pH were prepared using HCl (0.1 mol/L) and NaOH (0.1 mol/L) solutions. Swelling behavior of the sample in four different saline solutions (0.10 mol/L $CaCl_2$, NaCl, and KCl and Na_2SO_4) and distilled water was also assessed to identify the effect of different ions on swelling capacity and fertilizer release.

To do so, 2 g of nanocomposite powder was transferred to nylon bags, and soaked in 150 mL of the swelling solution at room temperature until the samples reached swelling equilibrium. At different time intervals, 2, 5, 10, 15, 20, 30, 45, 60, 90, 120, 180, 240, 360 and 480 min, the bags were removed from the swelling medium and weighed. The equilibrium water absorbency of each sample at time t (S_t, g/g) was defined as the gram of water uptake per gram of sample (See Eq. (1)).

$$S_t = \frac{M - M_0}{M_0} \tag{1}$$

where M_0 and M are the mass of dried and swollen products at time t, respectively.

3.2. Swelling kinetics

To identify the swelling behavior of the nanocomposite hydrogel, Schott's second-order swelling kinetics model was used (Yin et al., 2010).

$$\frac{t}{S_t} = \frac{1}{K_{is}} + \frac{1}{S_{eq}} t \tag{2}$$

where S_t (g/g) is the water absorption capacity at any time t (s) while S_{eq} (g/g) stands for the theoretical equilibrium water absorption; and K_{is} (g/g s) represents a constant for the initial swelling rate. By plotting t/S_t *versus* t, a straight line with good linear correlation coefficient was obtained (Table 1) which indicated that the swelling kinetic of the nanocomposite hydrogel followed Schott's second-order swelling kinetics model. Moreover, S_{eq} and K_{is} were calculated through these fitted straight line which simply the slope and intercept.

3.3. Fertilizer release at various pHs and salt solutions

The release behavior of NP fertilizers from BPC-gPAA/PVA/LDH at various pHs and salt solutions was determined as follows: 1.0 g dried hydrogel was soaked in 1000 mL release solution in a bottle equipped with a stopper. At predetermined time intervals, 3 mL of solution was drawn out from the bottle to detect the amount of released fertilizer using UV–visible spectrophotometry. The percentage of fertilizer release was calculated using Eq. (3):

$$\textit{Fertilizer release } (\%) = \frac{0.5 \times C_i}{0.2 \times C} \times 100\% \tag{3}$$

where Ci (g/L) and C (g/g) represent the contents of nitrogen and phosphorus in immersion solution and samples, respectively. In this work, C (nitrogen) = 0.061 g/g; C (phosphorus) = 0.021 g/g.

Table 1 Swelling kinetic parameters for BPC-g-PAA/PVA/LDH/NP nanocomposite hydrogel in different salt solutions.

Condition		S_{eq}(g/g)	K_{is} (g/gs)	R^2
Distilled Water	–	233.61	0.6418	0.9979
Ionic solution	$CaCl_2$	–	–	–
	NaCl	110.75	0.3147	0.9986
	KCl	96.53	0.2713	0.9981
	Na_2SO_4	76.02	0.1149	0.9975

3.4. Water retention studies with and without SRF formulation

Water-retention of fertilizer containing BPC-gPAA, BPC-gPAA/PVA and BPC-gPAA/PVA/LDH nanocomposites in loamy sand soil was investigated by mixing 2.0 g of dry sample of hydrogel formulation and 100 g of dry soil in a plastic cup. Then, 50 mL distilled water was added to the cup and weighed (W_0). A control study was also performed using 100 g of dry soil without hydrogel formulation (W_c). The cups were maintained at room temperature and weighed every day (W_t) up to 30 days. Finally, the percentage of water retention (WR %) of soil was calculated using Eq. (4):

$$WR\% = \left(\frac{W_t - W_c}{W_0 - W_c}\right) \times 100 \quad (4)$$

4. Results and discussion

4.1. XRD analysis of LDH nanosheets

Fig. 1 shows the XRD pattern of the Mg-Al LDH nanosheet. The characteristic peaks of layered structures were observed belonging to the 003 and 006 planes (sharp and symmetric reflections) and the 015 and 018 planes (broad and asymmetric reflections). The 003 d-spacing value was 7.91 Å. The high intensity of all characteristic peaks for Mg-Al LDH confirmed the high crystallinity of this LDH.

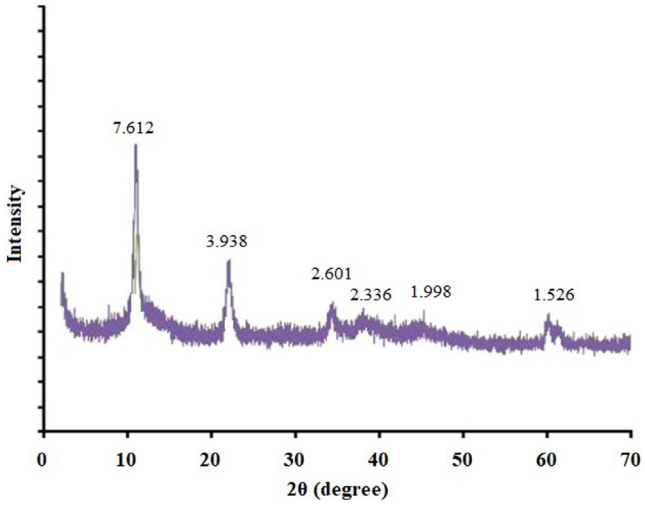

Fig. 1 The XRD pattern of chloride form Mg-Al LDH nanosheets.

4.2. FTIR spectra analysis

Fig. 2 represents the FTIR spectra of pure BPC and BPC-gPAA/PVA/LDH nanocomposite. The common absorption peaks of cellulose were observed in the spectrum of BPC, including the peak at 1054 cm^{-1} associated with b-1,4-glycosidic bond, 1426 cm^{-1} caused by stretching vibration of carbonyl, 1644 cm^{-1} caused by stretching vibration of C═O group of amide I band, 2914 cm^{-1} attributed to methylene group and 3401 cm^{-1} corresponding to stretching vibration of O—H (Tibolla et al., 2018).

In the spectrum of BPC-gPAA/PVA/LDH composite, the peaks at 1171 cm^{-1} and 1669 cm^{-1} attributed to the bending vibration of N—H and the C═O group of acrylamide unit, indicated the formation of acrylamides due to the condensation reaction between urea and acrylic acid. The peaks at 1628 cm^{-1} and 3435 cm^{-1} correspond to C═O and N—H stretching in C═O—NH_2 unit, respectively (Amin et al., 2012). The presence of peaks at 1388 cm^{-1} and 1562 cm^{-1}, attributed to the stretching of C—O—C and the —COO – groups in AA, respectively, could be due to the partially transformation of —COOH groups of AA to —COO – groups (Spagnol et al., 2012). Additionally, the peaks located at 520 cm^{-1} (bending vibration), 2919 cm^{-1} (stretching vibration of C—H in acrylate unit) confirmed the graft copolymerization of hydroxyl groups of AA and BPC

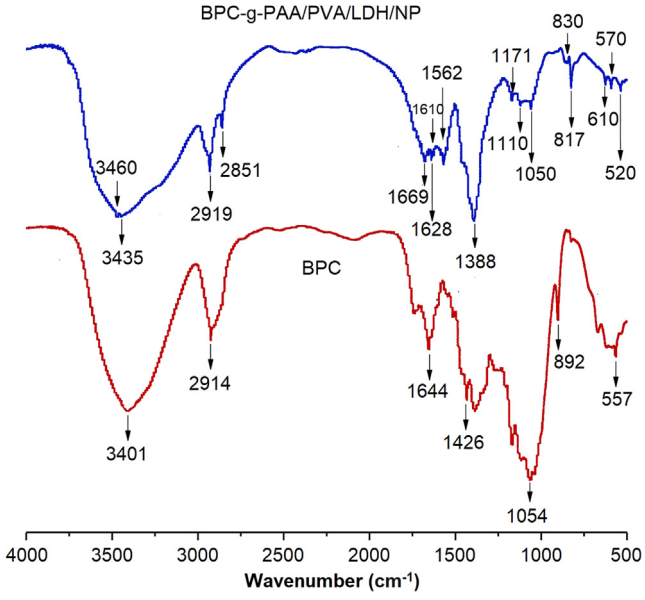

Fig. 2 The FTIR spectra of BPC and BPC-g-PAA/PVA/LDH/NP.

(Wu et al., 2012). The peaks at 1110 cm^{-1} and 817 cm^{-1} caused by stretching vibration of P═O and P─O, respectively, indicated the presence of di-potassium hydrogen phosphate in the composite in its original form (Zhan et al., 2004).

The peaks at 830, 610 and 570 cm^{-1} correspond to the vibration modes of LDH lattice (νM─O─M, νM─O). Moreover, other characteristic bands of LDH were observed at 3460 cm^{-1} (stretching), 1610 cm^{-1} (deformation) and 1050 cm^{-1} (bending) which are attributed to the vibration modes of the hydroxyl groups of LDH layers (Olfs et al., 2009; Everaert et al., 2016). In conclusion, a copolymer formed between AA and BPC which further formed a semi-IPNs composite with PVA. The fertilizers, nitrogen and phosphorus, were incorporated within the hydrogel via chemical reaction and physical entrapment.

4.3. Surface morphology analysis

SEM technique was used to observe the surface morphologies of BPC and BPC-gPAA/PVA/LDH (Fig. 3). As seen in Fig. 2a, BPC has a dense structure with relatively smooth surface, while BPC-gPAA/PVA/LDH (Fig. 3b) has a rough and highly porous surface, enhancing the water absorption and retention of the nanocomposite hydrogel product. The interconnected pores also delay the release of incorporated fertilizer into aqueous medium providing the slow release property for the nanocomposite hydrogel. The porous structure of nanocomposite hydrogel is the result of crosslinking and LDH nanoparticles incorporation.

4.4. Swelling and fertilizer release study at various pHs

The swelling capacity of fertilizer containing BPC-gPAA/PVA/LDH hydrogel varied as the pH of swelling medium changed, because the protonation extent of carboxyl groups of BPC was influenced by the pHs of swelling medium. As seen in Fig. 4, the swelling capacity showed an increasing trend up to pH 7, while it decreased instantly at pHs higher than 7. The pH-responsive swelling capacity of BPC-gPAA/PVA/LDH hydrogel was due to the protonation of carboxyl groups of BPC at acidic pHs which decreased anion-anion repulsion and at the same time, reinforced the hydrogen-bonding interaction between carboxylate groups. While by increasing pH up to 7, the protonation extent of carboxylate anions decreased and as a result, repulsive electrostatic forces increased; at the same time, the hydrogen bonding interaction between hydrophilic groups were weakened. Therefore, the water absorbency of BPC-gPAA/PVA/LDH hydrogel enhanced. However, at pHs higher than 7, additional Na^+ cations in the swelling medium created a screen effect which shielded the charges of carboxyl groups and consequently, weakened the efficient anion-anion electrostatic repulsion which led to the decrease of water absorption (Zhang et al., 2010).

As shown in Fig. 4(b) and (c), nitrogen and phosphorus fertilizers possessed completely opposite release profiles. As pH increased from 2 to 12, the release rate of nitrogen had a decreasing trend followed by an increase, while for phosphorus fertilizers, the release rate firstly increased and then declined. The formation of NH_4Cl from the reaction between acrylamide in BPC-gPAA/PVA/LDH with H ions could be the reason of the higher nitrogen release at low pH. While, in strongly acidic conditions, the transformation of carboxyl groups of BPC-gPAA/PVA/LDH into ─COOH decreased the repulsive forces between PO_3^{-4} and carboxyl resulting in the lower release of phosphorus. Additionally, the formation ─COOH at low pH enhanced the hydrogen bonding interactions, which had negative effect on the phosphate release. In an alkaline condition, the reaction between sodium ions and carboxyl groups reduces electrostatic repulsion between PO_3^{-4} and carboxyl which results in the lower release of phosphorus. On the contrary, nitrogen had a higher cumulative release amount in alkaline conditions due to the reaction between OH^- and acrylamide groups resulting in the yielding of NH_3.

4.5. Swelling and fertilizer release study at various salt solutions

The results of water absorption and fertilizer release kinetics of BPC-gPAA/PVA/LDH in various saline solutions ($CaCl_2$, NaCl, KCl and Na_2SO_4) are presented in Fig. 5. As seen in

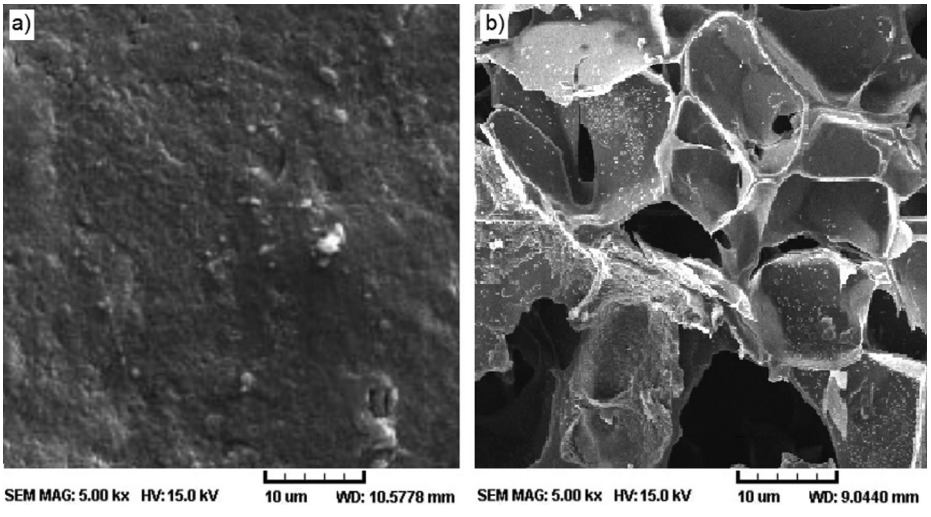

Fig. 3 SEM micrographs of (a) BPC and (b) BPC-g-PAA/PVA/LDH/NP.

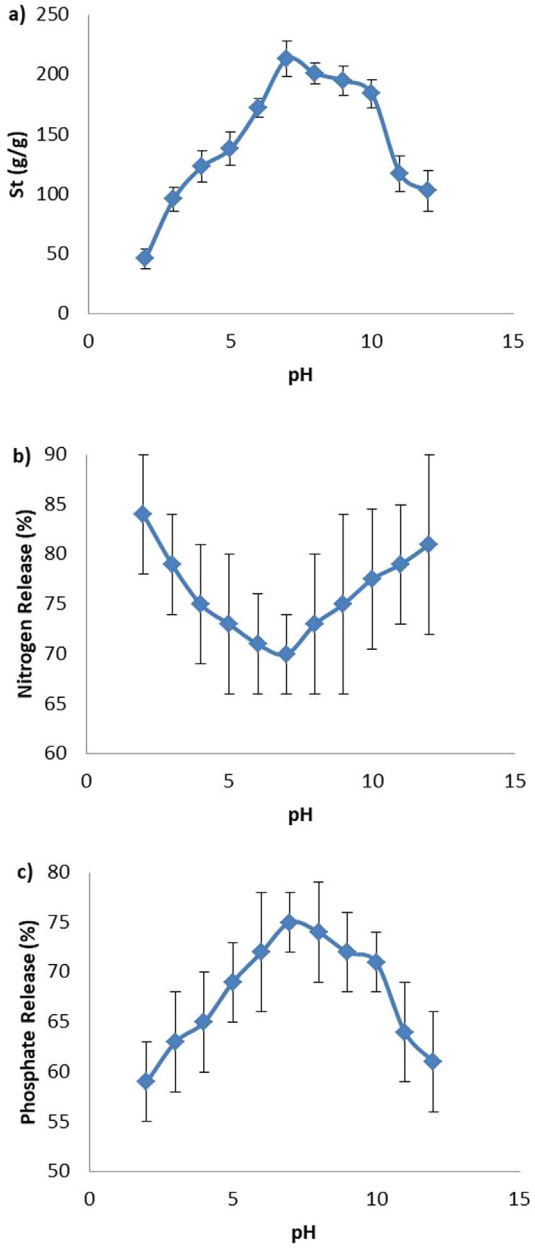

Fig. 4 (a) Swelling, (b) phosphorus release, and (c) nitrogen release behaviors of BPC-g-PAA/PVA/LDH nanocomposite hydrogel at the presence of various salt solutions.

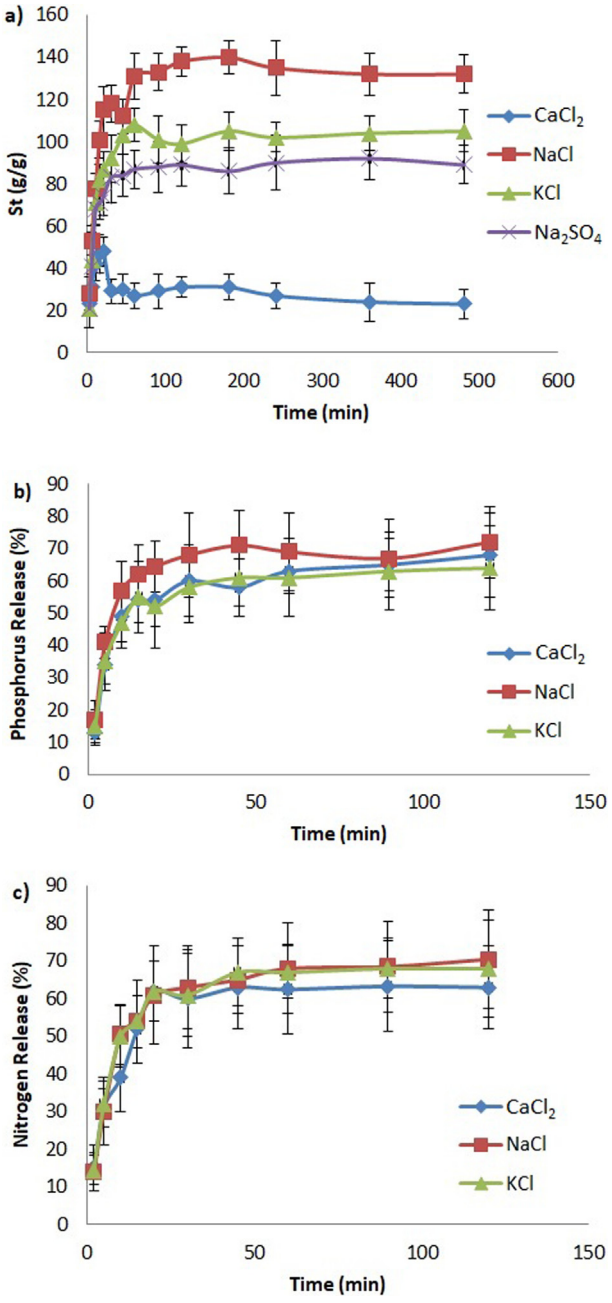

Fig. 5 (a) Swelling, (b) phosphorus release, and (c) nitrogen release behaviors of BPC-g-PAA/PVA/LDH nanocomposite hydrogel at different pHs.

Fig. 5a, the swelling rate and capacity of composite hydrogel decreased when additional ions existed in the solution. According to the data presented in Table 1, S_{eq} and K_{is} in saline solutions were lower compared to those in distilled water. This observation is common in ionic hydrogels static swelling experiments (Olad et al., 2017) which could arise from the charge screening effect (CSE) of the additional cations. CSE could also decrease the anion-anion electrostatic repulsion. Also, the presence of additional ions in the salt solutions decreases the gradient of osmotic pressure between the hydrogel network and the release solution. However, the release of fertilizers increased in the presence of cations due to the competitive adsorption and complex formation, *etc*.

The water absorption of hydrogel in KCl, NaCl, and Na_2SO_4 solutions increased over time (Fig. 4a), till it reached the equilibrium after 45 min, averagely. While in $CaCl_2$ solution, the swelling firstly increased and then declined. The swelling capacity of hydrogel in the different saline solutions was as follows: The highest swelling occurred in NaCl solution, then in KCl and Na_2SO_4 and $CaCl_2$ respectively. Therefore, Na^+ cation had the weakest effect on swelling, then K^+ and Ca^{2+}, respectively. The stronger effect of bivalent cation (Ca^{2+}) could be due to the interaction between Ca^{2+} ion and carboxyl groups of BPC-gPAA/PVA/LDH and formation of complexes between those (Lee & Yang, 2004). The forma-

tion of intermolecular and intramolecular complexes reduces the water absorbency of the hydrogel (Bao et al., 2011). Furthermore, the presence of Cl^- ions in in $CaCl_2$ solution decreases the osmotic pressure gradient which results in a lower water absorption by hydrogel. The water absorption of hydrogel in $CaCl_2$ solution dramatically decreased over time till it reached 23 g/g; which was the result of an overshooting effect. Although, the decrease in water absorption capacity of hydrogel was partially due to the formation of complexes between Ca^{2+} ions and carboxyl groups and thus enhancement of crosslinking degree of hydrogel; but the expansion of hydrogel matrix in $CaCl_2$ solution was mainly the result of water penetration. Pseudo second-order swelling kinetics model was not considered for evaluating the swelling rate and capacity of hydrogel due to the special swelling pattern of BPC-gPAA/PVA/LDH in $CaCl_2$ solution. The swelling ratio of hydrogel was higher when subjected to NaCl solution (Na^+) compared to KCl solution (K^+), which was due to the smaller size of Na^+ ions and thus their easier penetration into the internal matrix of the semi-IPNs hydrogel causing lower osmotic pressure difference.

According to the results of Table 1 for anions, water absorbency was more affected by monovalent anions (Cl^-) than divalent anions (SO_2^{-4}). This also could be due to the higher ionic strength of SO_2^{-4} which creates greater osmotic pressure gradient between the internal hydrogel network and the external solution. As seen in Fig. 4(b) and (c), the effects of different cations on the release kinetics of fertilizers were ordered as follows: $Na^+ > K^+ > Ca^{2+}$. The fertilizers release was higher when subjected to monovalent cations than that of bivalent cations which was in agreement with the results of water absorbency. As explained before, during swelling of hydrogel, Ca^{2+} ions enter the hydrogel matrix and then produce complexes with the carboxyl groups of BPC-gPAA/PVA/LDH, resulting in a greater crosslinking degree and consequently slower fertilizers release. Regarding the order of $Na^+ > K^+$, as mentioned before the swelling and fertilizers release were dependent to the size of monovalent cation. N^+ ions with a smaller size than K^+, could enter the hydrogel network easier and consequently, compete with fertilizers molecules for adsorption sites on hydrogel, and simultaneously, decrease the osmotic pressure difference which results in the faster release rate of fertilizers.

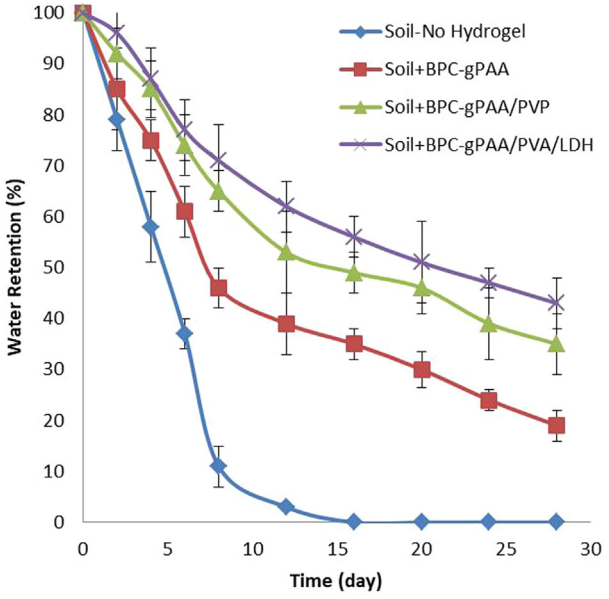

Fig. 6 Effect of fertilizer containing BPC-g-PAA, BPC-g-PAA/PVA and BPC-g-PAA/PVA/LDH nanocomposite hydrogel on water retention of sand soil.

4.6. Swelling kinetics

As shown in Figs. 4(a) and 5(a), the nanocomposite hydrogel at various salt solutions had a biphasic swelling profile. At first 45–60 min, the swelling rate was fast, and then it reached an early equilibrium state. The result of Table 1 confirmed that the swelling behavior of the nanocomposite hydrogel at various salt solutions matched the Schott's second-order swelling kinetics model, because the plot of t/S_t *versus* t forms a straight line with a good linear correlation coefficient. S_{eq} and K_{is} are calculated through the intercept and slope obtained by the fitted straight lines.

4.7. Water retention behavior of BPC-gPAA/PVA/LDH/NP in soil

Water retention behavior of fertilizer containing BPC-gPAA, BPC-gPAA/PVA and BPC-gPAA/PVA/LDH nanocomposite in loamy sand soil is presented in Fig. 6. By adding the hydrogel products into loamy sand soil, its water retention increased for a longer period of time, while the water content of soil sample without hydrogel completely vaporized after 16 days. Furthermore, the water retention of soil containing BPC-gPAA/PVA and BPC-gPAA/PVA/LDH was better than soil containing neat BPC-gPAA. This result indicated that incorporation of LDH nanoparticles and PVA in hydrogel matrix improved its water retention property (Ribeiro et al., 2014). Therefore, the use of fertilizer containing BPC-gPAA/PVA/LDH nanocomposite hydrogel in soil can extend the irrigation time and improve the agriculture and horticulture in drylands.

5. Conclusion

A novel pH-sensitive CRF nanocomposite containing BPC-g-PAA/PVA hydrogel, LDH nanoparticles and NP fertilizers was synthesized via graft solution polymerization. The successful grafting of BPC chains with AA monomers was confirmed by SEM and FTIR analysis. The BPC-g-PAA/PVA/LDH/NP nanocomposite possessed a good pH and salt sensitive swelling behavior and fertilizer release. Nitrogen fertilizer had a faster release rate at both strong alkaline or strong acid conditions and compared with neutral condition, while the highest phosphorus release occurred at pH 7. The swelling kinetic of the CRF nanocomposite hydrogel followed a Schott's second order equation. The swelling was affected by different ions by the order of $Ca^{2+} < K^+ < Na^+$ for cations and $SO_2^{-4} < Cl^-$ for anions, respectively. However, the hydrogel had a better swelling in neutral condition. Furthermore, the nanocomposite hydrogel significantly improved the water retention of loamy sand soil. These results suggest that this novel CRF BPC-gPAA/PVA/LDH/NP nanocomposite hydrogel can improve water conservation and also serve as a promising fertilizer carrier in agricultural applications.

Declaration of Competing Interest

The authors declare that they have no known competing financial interests or personal relationships that could have appeared to influence the work reported in this paper.

References

Amin, M.C.I.M., Ahmad, N., Halib, N., Ahmad, I., 2012. Synthesis and characterization of thermo-and pH-responsive bacterial cellulose/acrylic acid hydrogels for drug delivery. Carbohydr. Polym. 88 (2), 465–473.

Arif, M., Yasin, G., Luo, L., Ye, W., Mushtaq, M.A., Fang, X., Yan, D., 2020. Hierarchical hollow nanotubes of NiFeV-layered double hydroxides@ CoVP heterostructures towards efficient, pH-universal electrocatalytical nitrogen reduction reaction to ammonia. Appl. Catal. B 265, 118559.

Bao, Y., Ma, J., Li, N., 2011. Synthesis and swelling behaviors of sodium carboxymethyl cellulose-g-poly (AA-co-AM-co-AMPS)/MMT superabsorbent hydrogel. Carbohydr. Polym. 84 (1), 76–82.

Bernardo, M.P., Moreira, F.K., Ribeiro, C., 2017. Synthesis and characterization of eco-friendly Ca-Al-LDH loaded with phosphate for agricultural applications. Appl. Clay Sci. 137, 143–150.

Dai, H., Huang, H., 2017. Enhanced swelling and responsive properties of pineapple peel carboxymethyl cellulose-g-poly (acrylic acid-co-acrylamide) superabsorbent hydrogel by the introduction of carclazyte. J. Agric. Food. Chem. 65 (3), 565–574.

Díaz-Pinés, E., Molina-Herrera, S., Dannenmann, M., Braun, J., Haas, E., Willibald, G., Aust, C., 2017. Nitrate leaching and soil nitrous oxide emissions diminish with time in a hybrid poplar short-rotation coppice in southern Germany. GCB Bioenergy 9 (3), 613–626.

Erisman, J.W., Bleeker, A., Galloway, J., Sutton, M.S., 2007. Reduced nitrogen in ecology and the environment. Environ. Pollut. 150 (1), 140–149.

Essawy, H.A., Ghazy, M.B., Abd El-Hai, F., Mohamed, M.F., 2016. Superabsorbent hydrogels via graft polymerization of acrylic acid from chitosan-cellulose hybrid and their potential in controlled release of soil nutrients. Int. J. Biol. Macromol. 89, 144–151.

Everaert, M., Warrinnier, R., Baken, S., Gustafsson, J.P., De Vos, D., Smolders, E., 2016. Phosphate-exchanged Mg–Al layered double hydroxides: a new slow release phosphate fertilizer. ACS Sustain. Chem. Eng. 4 (8), 4280–4287.

Fekete, T., Borsa, J., Takács, E., Wojnárovits, L., 2016. Synthesis of carboxymethylcellulose/acrylic acid hydrogels with superabsorbent properties by radiation-initiated crosslinking. Radiat. Phys. Chem. 124, 135–139.

Fekete, T., Borsa, J., Takács, E., Wojnárovits, L., 2017. Synthesis and characterization of superabsorbent hydrogels based on hydroxyethylcellulose and acrylic acid. Carbohydr. Polym. 166, 300–308.

Gao, R., Yan, D., Evans, D.G., Duan, X., 2017. Layer-by-layer assembly of long-afterglow self-supporting thin films with dual-stimuli-responsive phosphorescence and antiforgery applications. Nano Res. 10 (10), 3606–3617.

Gao, R., Yan, D., 2018. Fast formation of single-unit-cell-thick and defect-rich layered double hydroxide nanosheets with highly enhanced oxygen evolution reaction for water splitting. Nano Res. 11 (4), 1883–1894.

González, M.E., Cea, M., Medina, J., González, A., Diez, M.C., Cartes, P., Navia, R., 2015. Evaluation of biodegradable polymers as encapsulating agents for the development of a urea controlled-release fertilizer using biochar as support material. Sci. Total Environ. 505, 446–453.

Guilherme, M.R., Aouada, F.A., Fajardo, A.R., Martins, A.F., Paulino, A.T., Davi, M.F., Muniz, E.C., 2015. Superabsorbent hydrogels based on polysaccharides for application in agriculture as soil conditioner and nutrient carrier: A review. Eur. Polym. J. 72, 365–385.

Hatami, H., Fotovat, A., Halajnia, A., 2018. Comparison of adsorption and desorption of phosphate on synthesized Zn-Al LDH by two methods in a simulated soil solution. Appl. Clay Sci. 152, 333–341.

Hibino, T., 2010. New nanocomposite hydrogels containing layered double hydroxide. Appl. Clay Sci. 50 (2), 282–287.

Lee, W.F., Yang, L.G., 2004. Superabsorbent polymeric materials. XII. Effect of montmorillonite on water absorbency for poly (sodium acrylate) and montmorillonite nanocomposite superabsorbents. J. Appl. Polym. Sci. 92 (5), 3422–3429.

Lewandowska-Łańcucka, J., Fiejdasz, S., Rodzik, Ł., Kozieł, M., Nowakowska, M., 2015. Bioactive hydrogel-nanosilica hybrid materials: a potential injectable scaffold for bone tissue engineering. Biomed. Mater. 10, (1) 015020.

Li, D.P., Wu, Z.J., 2008. Impact of chemical fertilizers application on soil ecological environment. Ying yong sheng tai xue bao = J. Appl. Ecol. 19 (5), 1158–1165.

Li, W., Guo, S., Liu, H., Zhai, L., Wang, H., Lei, Q., 2018. Comprehensive environmental impacts of fertilizer application vary among different crops: Implications for the adjustment of agricultural structure aimed to reduce fertilizer use. Agric. Water Manage. 210, 1–10.

Mahfoudhi, N., Boufi, S., 2016. Poly (acrylic acid-co-acrylamide)/cellulose nanofibrils nanocomposite hydrogels: effects of CNFs content on the hydrogel properties. Cellulose 23 (6), 3691–3701.

Majeed, Z., Ramli, N.K., Mansor, N., Man, Z., 2015. A comprehensive review on biodegradable polymers and their blends used in controlled-release fertilizer processes. Rev. Chem. Eng. 31 (1), 69–95.

McLaughlin, J.R., Abbott, N.L., Guymon, C.A., 2018. Responsive superabsorbent hydrogels via photopolymerization in lyotropic liquid crystal templates. Polymer 142, 119–126.

Mishra, G., Dash, B., Pandey, S., 2018. Layered double hydroxides: A brief review from fundamentals to application as evolving biomaterials. Appl. Clay Sci. 153, 172–186.

Nath, J., Dolui, S.K., 2018. Synthesis of carboxymethyl cellulose-g-poly (acrylic acid)/LDH hydrogel for in vitro controlled release of vitamin B12. Appl. Clay Sci. 155, 65–73.

Obermeier, M.M., Gnädinger, F., Raj, A.C.D., Obermeier, W.A., Schmid, C.A., Balàzs, H., Schröder, P., 2020. Under temperate climate, the conversion of grassland to arable land affects soil nutrient stocks and bacteria in a short term. Sci. Total Environ. 703, 135494.

Olad, A., Gharekhani, H., Mirmohseni, A., Bybordi, A., 2017. Synthesis, characterization, and fertilizer release study of the salt and pH-sensitive NaAlg-g-poly (AA-co-AAm)/RHA superabsorbent nanocomposite. Polym. Bull. 74 (8), 3353–3377.

Olfs, H.W., Torres-Dorante, L.O., Eckelt, R., Kosslick, H., 2009. Comparison of different synthesis routes for Mg–Al layered double hydroxides (LDH): Characterization of the structural phases and anion exchange properties. Appl. Clay Sci. 43 (3–4), 459–464.

Peng, N., Wang, Y., Ye, Q., Liang, L., An, Y., Li, Q., Chang, C., 2016. Biocompatible cellulose-based superabsorbent hydrogels with antimicrobial activity. Carbohydr. Polym. 137, 59–64.

Pu, S.H.E.N., Li, D.C., Gao, J.S., Xu, M.G., Wang, B.R., Hou, X.J., 2011. Effects of long-term application of sulfur-containing and chloride-containing chemical fertilizers on rice yield and its components. Agric. Sci. China 10 (5), 747–753.

Rassu, M., Alzari, V., Nuvoli, D., Nuvoli, L., Sanna, D., Sanna, V., Mariani, A., 2017. Semi-interpenetrating polymer networks of methyl cellulose and polyacrylamide prepared by frontal polymerization. J. Polym. Sci., Part A: Polym. Chem. 55 (7), 1268–1274.

Ribeiro, L.N., Alcântara, A.C., Darder, M., Aranda, P., Araújo-Moreira, F.M., Ruiz-Hitzky, E., 2014. Pectin-coated chitosan–LDH bionanocomposite beads as potential systems for colon-targeted drug delivery. Int. J. Pharm. 463 (1), 1–9.

Ros, G.H., Van Rotterdam, A.M.D., Bussink, D.W., Bindraban, P.S., 2016. Selenium fertilization strategies for bio-fortification of food: an agro-ecosystem approach. Plant Soil 404 (1–2), 99–112.

Saiah, F.B.D., Su, B.L., Bettahar, N., 2009. Nickel–iron layered double hydroxide (LDH): textural properties upon hydrothermal treatments and application on dye sorption. J. Hazard. Mater. 165 (1–3), 206–217.

Salmawi, K.M.E., El-Naggar, A.A., Ibrahim, S.M., 2018. Gamma irradiation synthesis of carboxymethyl cellulose/acrylic acid/clay superabsorbent hydrogel. Adv. Polym. Technol. 37 (2), 515–521.

Spagnol, C., Rodrigues, F.H., Pereira, A.G., Fajardo, A.R., Rubira, A.F., Muniz, E.C., 2012. Superabsorbent hydrogel composite made of cellulose nanofibrils and chitosan-graft-poly (acrylic acid). Carbohydr. Polym. 87 (3), 2038–2045.

Sun, H., Zhang, H., Min, J., Feng, Y., Shi, W., 2016. Controlled-release fertilizer, floating duckweed, and biochar affect ammonia volatilization and nitrous oxide emission from rice paddy fields irrigated with nitrogen-rich wastewater. Paddy Water Environ, 14 (1), 105–111.

Thompson, C.B., Chatterjee, S., Korley, L.T., 2019. Gradient supramolecular interactions and tunable mechanics in polychaete jaw inspired semi-interpenetrating networks. Eur. Polym. J. 116, 201–209.

Tian, R., Zhang, S., Li, M., Zhou, Y., Lu, B., Yan, D., Duan, X., 2015. Localization of Au nanoclusters on layered double hydroxides nanosheets: confinement-induced emission enhancement and temperature-responsive luminescence. Adv. Funct. Mater. 25 (31), 5006–5015.

Tibolla, H., Pelissari, F.M., Rodrigues, M.I., Menegalli, F.C., 2017. Cellulose nanofibers produced from banana peel by enzymatic treatment: Study of process conditions. Ind. Crops Prod. 95, 664–674.

Tibolla, H., Pelissari, F.M., Martins, J.T., Vicente, A.A., Menegalli, F. C., 2018. Cellulose nanofibers produced from banana peel by chemical and mechanical treatments: characterization and cytotoxicity assessment. Food Hydrocolloids 75, 192–201.

Wang, J., Chen, H., Xiao, Y., Yu, X., Li, X., 2019. PAMPS/PVA/MMT Semi-interpenetrating polymer network hydrogel electrolyte for solid-state supercapacitors. Int. J. Electrochem. Sci. 14 (1), 1817–1829.

Wang, Q., O'Hare, D., 2012. Recent advances in the synthesis and application of layered double hydroxide (LDH) nanosheets. Chem. Rev. 112 (7), 4124–4155.

Wu, F., Zhang, Y., Liu, L., Yao, J., 2012. Synthesis and characterization of a novel cellulose-g-poly (acrylic acid-co-acrylamide) superabsorbent composite based on flax yarn waste. Carbohydr. Polym. 87 (4), 2519–2525.

Xu, J., Fan, L., Xie, Y., Wu, G., 2019. Recycling-equilibrium strategy for phosphogypsum pollution control in phosphate fertilizer plants. J. Cleaner Prod. 215, 175–197.

Yao, C., Liu, Z., Yang, C., Wang, W., Ju, X.J., Xie, R., Chu, L.Y., 2016. Smart hydrogels with inhomogeneous structures assembled using nanoclay-cross-linked hydrogel subunits as building blocks. ACS Appl. Mater. Interfaces 8 (33), 21721–21730.

Yin, Y., Lv, X., Tu, H., Xu, S., Zheng, H., 2010. Preparation and swelling kinetics of pH-sensitive photocrosslinked hydrogel based on carboxymethyl chitosan. J. Polym. Res. 17 (4), 471–479.

You, J., Xie, S., Cao, J., Ge, H., Xu, M., Zhang, L., Zhou, J., 2016. Quaternized chitosan/poly (acrylic acid) polyelectrolyte complex hydrogels with tough, self-recovery, and tunable mechanical properties. Macromolecules 49 (3), 1049–1059.

Zhan, F., Liu, M., Guo, M., Wu, L., 2004. Preparation of superabsorbent polymer with slow-release phosphate fertilizer. J. Appl. Polym. Sci. 92 (5), 3417–3421.

Zhang, B., Cui, Y., Yin, G., Li, X., You, Y., 2010. Synthesis and swelling properties of hydrolyzed cottonseed protein composite superabsorbent hydrogel. Int. J. Polym. Mater. 59 (12), 1018–1032.